



# Time course of phosphorylated-tau181 in blood across the Alzheimer's disease spectrum

Alexis Moscoso,<sup>1,2</sup> Michel J. Grothe,<sup>1,2,3</sup> Nicholas J. Ashton,<sup>1,2,4,5</sup>  Thomas K. Karikari,<sup>1</sup> Juan Lantero Rodriguez,<sup>1</sup>  Anniina Snellman,<sup>1,6</sup> Marc Suárez-Calvet,<sup>7,8,9,10</sup> Henrik Zetterberg,<sup>1,11,12,13</sup> Kaj Blennow<sup>1,11</sup> and Michael Schöll<sup>1,2,12</sup> for the Alzheimer's Disease Neuroimaging Initiative<sup>†</sup>

<sup>†</sup>Data used in preparation of this article were obtained from the Alzheimer's Disease Neuroimaging Initiative (ADNI) database (<http://adni.loni.usc.edu/>). As such, the investigators within the ADNI contributed to the design and implementation of ADNI and/or provided data but did not participate in analysis or writing of this report. A complete listing of ADNI investigators can be found at: [http://adni.loni.usc.edu/wp-content/uploads/how\\_to\\_apply/ADNI\\_Acknowledgement\\_List.pdf](http://adni.loni.usc.edu/wp-content/uploads/how_to_apply/ADNI_Acknowledgement_List.pdf)

See Tijms and Teunissen (doi:10.1093/brain/awaa422) for a scientific commentary on this article.

Tau phosphorylated at threonine 181 (p-tau181) measured in blood plasma has recently been proposed as an accessible, scalable, and highly specific biomarker for Alzheimer's disease. Longitudinal studies, however, investigating the temporal dynamics of this novel biomarker are lacking. It is therefore unclear when in the disease process plasma p-tau181 increases above physiological levels and how it relates to the spatiotemporal progression of Alzheimer's disease characteristic pathologies. We aimed to establish the natural time course of plasma p-tau181 across the sporadic Alzheimer's disease spectrum in comparison to those of established imaging and fluid-derived biomarkers of Alzheimer's disease. We examined longitudinal data from a large prospective cohort of elderly individuals enrolled in the Alzheimer's Disease Neuroimaging Initiative (ADNI) ( $n = 1067$ ) covering a wide clinical spectrum from normal cognition to dementia, and with measures of plasma p-tau181 and an <sup>18</sup>F-florbetapir amyloid- $\beta$  PET scan at baseline. A subset of participants ( $n = 864$ ) also had measures of amyloid- $\beta_{1-42}$  and p-tau181 levels in CSF, and another subset ( $n = 298$ ) had undergone an <sup>18</sup>F-flortaucipir tau PET scan 6 years later. We performed brain-wide analyses to investigate the associations of plasma p-tau181 baseline levels and longitudinal change with progression of regional amyloid- $\beta$  pathology and tau burden 6 years later, and estimated the time course of changes in plasma p-tau181 and other Alzheimer's disease biomarkers using a previously developed method for the construction of long-term biomarker temporal trajectories using shorter-term longitudinal data. Smoothing splines demonstrated that earliest plasma p-tau181 changes occurred even before amyloid- $\beta$  markers reached abnormal levels, with greater rates of change correlating with increased amyloid- $\beta$  pathology. Voxel-wise PET analyses yielded relatively weak, yet significant, associations of plasma p-tau181 with amyloid- $\beta$  pathology in early accumulating brain regions in cognitively healthy individuals, while the strongest associations with amyloid- $\beta$  were observed in late accumulating regions in patients with mild cognitive impairment. Cross-sectional and particularly longitudinal measures of plasma p-tau181 were associated with widespread cortical tau aggregation 6 years later, covering temporoparietal regions typical for neurofibrillary tangle distribution in Alzheimer's disease. Finally, we estimated that plasma p-tau181 reaches abnormal levels  $\sim 6.5$  and 5.7 years after CSF and PET measures of amyloid- $\beta$ , respectively, following similar dynamics as CSF p-tau181. Our findings suggest that plasma p-tau181 increases are associated with the presence of widespread cortical amyloid- $\beta$  pathology and with prospective Alzheimer's disease typical tau aggregation, providing clear implications for the use of this novel blood biomarker as a diagnostic and screening tool for Alzheimer's disease.

Received July 12, 2020. Revised September 15, 2020. Accepted September 20, 2020. Advance access publication November 30, 2020

© The Author(s) (2020). Published by Oxford University Press on behalf of the Guarantors of Brain.

This is an Open Access article distributed under the terms of the Creative Commons Attribution Non-Commercial License (<http://creativecommons.org/licenses/by-nc/4.0/>), which permits non-commercial re-use, distribution, and reproduction in any medium, provided the original work is properly cited. For commercial re-use, please contact [journals.permissions@oup.com](mailto:journals.permissions@oup.com)

- 1 Department of Psychiatry and Neurochemistry, Institute of Neuroscience and Physiology, The Sahlgrenska Academy, University of Gothenburg, Sweden
- 2 Wallenberg Centre for Molecular and Translational Medicine, University of Gothenburg, Sweden
- 3 Unidad de Trastornos del Movimiento, Instituto de Biomedicina de Sevilla (IBiS), Hospital Universitario Virgen del Rocío/CSIC/Universidad de Sevilla, Sevilla, Spain
- 4 King's College London, Institute of Psychiatry, Psychology and Neuroscience, Maurice Wohl Clinical Neuroscience Institute, London, UK
- 5 NIHR Biomedical Research Centre for Mental Health and Biomedical Research Unit for Dementia at South London and Maudsley NHS Foundation, London, UK
- 6 Turku PET Centre, University of Turku, FI-20520 Turku, Finland
- 7 Barcelonaβeta Brain Research Center (BBRC), Pasqual Maragall Foundation, Barcelona, Spain
- 8 IMIM (Hospital del Mar Medical Research Institute), Barcelona, Spain
- 9 Servei de Neurologia, Hospital del Mar, Barcelona, Spain
- 10 Centro de Investigación Biomédica en Red de Fragilidad y Envejecimiento Saludable (CIBERFES), Madrid, Spain
- 11 Clinical Neurochemistry Laboratory, Sahlgrenska University Hospital, Mölndal, Sweden
- 12 Department of Neurodegenerative Disease, UCL Queen Square Institute of Neurology, University College London, London, UK
- 13 UK Dementia Research Institute at University College London, London, UK

Correspondence to: Michael Schöll, PhD  
 Sahlgrenska University Hospital, MedTech  
 West 10B, 413 45 Gothenburg, Sweden  
 E-mail: michael.scholl@neuro.gu.se

**Keywords:** Alzheimer's disease; blood biomarkers; tau; positron emission tomography; cerebrospinal fluid

**Abbreviations:** ADNI = Alzheimer's Disease Neuroimaging Initiative; FBP = <sup>18</sup>F-florbetapir; FTP = <sup>18</sup>F-flortaucipir; MCI = mild cognitive impairment; NFT = neurofibrillary tangle; p-tau181 = tau phosphorylated at threonine 181; SUVR = standardized uptake value ratio

## Introduction

Non-physiological accumulation of amyloid- $\beta$  peptides into extracellular plaques and aggregation of hyperphosphorylated tau protein into intracellular neurofibrillary tangles (NFT) constitute the neuropathological signature of Alzheimer's disease in the human brain (Hyman *et al.*, 2012). While the reliable detection of these pathological changes has traditionally been restricted to histopathological examination post-mortem, current PET and CSF biomarkers have enabled their accurate assessment *in vivo* (Blennow *et al.*, 2015; Schöll *et al.*, 2019). These biomarkers thus provide clinically relevant information for the detection and differential diagnosis of Alzheimer's disease (Dubois *et al.*, 2014; Ossenkoppele *et al.*, 2018), its progression (Hanseeuw *et al.*, 2019), as well as patient management (Rabinovici *et al.*, 2019), representing key modalities for obtaining an accurate, individualized picture of a patient's pathological profile. However, these specialized techniques are limited by relatively high costs, invasiveness, and/or limited availability in routine clinical settings, which hampers their generalized use in clinical practice.

Blood-based biomarkers for Alzheimer's disease have recently emerged as accessible, cost-effective, and relatively non-invasive tools for detecting Alzheimer's disease neuropathology *in vivo*, aiming at circumventing the aforementioned limitations of PET and CSF biomarkers (Zetterberg, 2019). Prior studies have found that blood plasma levels of the neuronal injury markers neurofilament light chain (NfL)

and total tau (t-tau) were significantly different in Alzheimer's disease patients compared to healthy control individuals (Mattsson *et al.*, 2016, 2017). They have also been shown to predict disease progression (Mielke *et al.*, 2017; Ashton *et al.*, 2019; Mattsson *et al.*, 2019), suggesting that these markers could potentially be used as simple and accessible tests for Alzheimer's disease. However, NfL and t-tau, whether derived from CSF or blood, are not specific for Alzheimer's disease (Ashton *et al.*, 2020). In contrast, blood plasma levels of amyloid- $\beta$ , with the amyloid- $\beta_{42/40}$  ratio reflecting brain amyloid- $\beta$  deposition, yielded high discrimination between amyloid- $\beta$ -positive (+) and amyloid- $\beta$ -negative (-) subjects, even at asymptomatic stages, as defined by validated approaches based on amyloid- $\beta$  PET (Nakamura *et al.*, 2018; Risacher *et al.*, 2019; Schindler *et al.*, 2019; Vergallo *et al.*, 2019). More recently, several reports have shown that tau phosphorylated at threonine 181 (p-tau181) in plasma increases gradually across the Alzheimer's disease continuum, accurately predicts cross-sectional brain amyloid- $\beta$  and tau pathology as assessed with PET, and reliably discriminates Alzheimer's disease from other neurodegenerative disorders (Mielke *et al.*, 2018; Benussi *et al.*, 2020; Janelidze *et al.*, 2020; Karikari *et al.*, 2020; Lantero Rodriguez *et al.*, 2020; Thijssen *et al.*, 2020). In familial Alzheimer's disease, plasma p-tau181 starts to increase ~16 years prior to estimated symptom onset (O'Connor *et al.*, 2020). In direct comparisons, plasma p-tau181 was more disease-specific and accurate than the other plasma-based biomarker candidates (Janelidze *et al.*, 2020; Karikari *et al.*,

2020). However, greatest accuracy for the prediction of amyloid- $\beta$  pathology was obtained when combining amyloid- $\beta$  and p-tau181 plasma biomarkers (Janelidze *et al.*, 2020), suggesting that both markers provide partly unique and complementary insights to underlying disease processes. In addition, two recent studies suggested highly promising diagnostic performance for plasma-derived tau phosphorylated at threonine 217 (Barthelemy *et al.*, 2020; Palmqvist *et al.*, 2020). Together, these studies support the potential of plasma biomarkers as a feasible and reliable first-line test for Alzheimer's disease in the clinic as well as in disease-modifying trials.

To date, apart from a relatively small familial Alzheimer's disease study (O'Connor *et al.*, 2020), available reports on plasma p-tau181 are limited to cross-sectional designs (Benussi *et al.*, 2020; Janelidze *et al.*, 2020; Karikari *et al.*, 2020; Thijssen *et al.*, 2020); therefore, the temporal dynamics of plasma p-tau181 changes across the spectrum of Alzheimer's disease, as well as its associations with the temporospatial progression of Alzheimer's disease pathology as measured by PET, remain unexplored. Addressing these questions is crucial to understand the full potential of plasma p-tau181 as an early predictor of Alzheimer's disease, as well as to more closely elucidate the specific aspects of Alzheimer's disease pathology reflected by this novel biomarker.

In the present study, we investigated the temporal trajectories of plasma p-tau181 across the spectrum of sporadic Alzheimer's disease and analysed their association with the spatiotemporal progression patterns of PET-measured amyloid- $\beta$  and tau pathology, as well as the trajectories of established CSF biomarkers. We examined a large, prospective cohort spanning the entire clinical Alzheimer's disease continuum with longitudinal plasma p-tau181 data as well as PET and CSF-based biomarkers. Under the hypothesis that plasma p-tau181 is a specific marker for Alzheimer's disease, our aims were to determine the natural course of plasma p-tau181 across the disease spectrum, investigating the specific events in the Alzheimer's disease cascade that most closely associate with dynamic changes in plasma p-tau181, and to estimate the time-point in this cascade at which plasma p-tau181 reaches abnormal levels.

## Material and methods

### Study design

Data were obtained from the Alzheimer's Disease Neuroimaging Initiative (ADNI) database (<http://adni.loni.usc.edu>). The ADNI is an ongoing observational study that was launched in 2003 as a public-private partnership, led by Principal Investigator Michael W. Weiner, MD. ADNI recruits participants at 57 sites in the USA and Canada. The primary goal of ADNI has been to test whether serial MRI, PET, other biological markers, and clinical and neuropsychological assessment can be combined to measure the progression of mild cognitive impairment (MCI) and early Alzheimer's disease. The study was approved by the Institutional Review Board (IRB) of all participating centres in ADNI. All study participants, or their study partners, provided written informed consent. For the present study, data were obtained from the Laboratory of Neuro Imaging (LONI) database in June 2020.

### Participants

We included all cognitively normal participants, patients with MCI, and patients with Alzheimer's disease dementia with at least one available plasma p-tau181 measurement and amyloid- $\beta$  PET scan ( $^{18}\text{F}$ -florbetapir; FBP) at baseline ( $n = 1067$ ). A subset of these participants ( $n = 864$ ) also had available measures of amyloid- $\beta_{1-42}$  and p-tau181 in CSF. ADNI participants were scheduled to undergo follow-up measurements of the aforementioned biomarkers. Additionally, another subset of study participants (156 cognitively normal, 138 MCI, and four Alzheimer's disease dementia) that continued in ADNI3, were scanned using tau PET imaging with  $^{18}\text{F}$ -flortaucipir (FTP) at an average of 6.1 years after the baseline visit. Characteristics of study participants are detailed in Table 1. ADNI inclusion criteria for the diagnostic cohorts have been described in detail elsewhere (Petersen *et al.*, 2010).

**Table 1** Demographic information of study participants

	Cognitively normal	MCI	Alzheimer's disease
<i>n</i>	359	518	186
Age, years	74.7 (6.7)	72.8 (7.9)	75.1 (7.8)
Sex, male/female	168/191	291/227	108/78
APOE $\epsilon 4$ carriers, <i>n</i> (% +)	102 (28)	241 (47)	122 (66)
MMSE	29 [24–30]	28 [24–30]	23 [9–26]
Amyloid- $\beta$ positive, <i>n</i> (%)	110 (31)	277 (53)	160 (86)
Centiloid (CL)	9.4 [–24.1 to 168.2]	30.2 [–29.7 to 188.8]	85.0 [–25.3 to 194.7]
Plasma p-tau181, pg/ml	13.6 [0.8–72.3]	15.8 [1.6–69.6]	23.2 [6.3–63.3]
CSF amyloid- $\beta_{1-42}$ , pg/ml	1291 [203–3462]	906 [248–3392]	624 [255–3139]
CSF p-tau181, pg/ml	19.6 [8.0–60.0]	22.8 [8.2–91.3]	33.4 [10.8–90]

Age is reported as mean (standard deviation). Continuous biomarker data are reported as median [range]. MMSE is reported as median [range]. MMSE = Mini-Mental State Examination.

## Plasma p-tau181 measurements

Blood samples were collected and processed according to the ADNI protocol (Kang *et al.*, 2015). Plasma p-tau181 concentrations were measured at the Clinical Neurochemistry Laboratory, University of Gothenburg (Mölndal, Sweden) using an assay developed in-house on a Simoa HD-X (Quanterix) instrument, as described previously in detail (Karikari *et al.*, 2020). In brief, the AT270 mouse monoclonal antibody (MN1050; Invitrogen) specific for the threonine-181 phosphorylation site, coupled to paramagnetic beads (103 207; Quanterix) was used for capture and the anti-tau mouse monoclonal antibody Tau12 (806 502; BioLegend), which binds the N-terminal epitope 6-QEFEVMDHAGT-18 on human tau protein, for detection. All of the available samples were analysed in a single batch. We identified four participants (0.4%) with outlier values of plasma p-tau181 levels that were discarded from subsequent analyses (Supplementary Fig. 1). Longitudinal blood sampling was performed approximately every year, over a median follow-up time of 2.9 years in 938 subjects.

## Image processing and analysis

Amyloid- $\beta$  PET imaging in ADNI was performed using FBP, with an injected dose of  $370 \pm 37$  MBq. PET images were acquired 50–70 min after injection of FBP using a dynamic protocol ( $4 \times 5$  min frames). Longitudinal amyloid- $\beta$  PET scans were acquired approximately every 2 years, with a median follow-up time of 4.0 years in 728 participants. Tau PET images were acquired 75–105 min after the injection of  $370 \pm 37$  MBq of FTP using a  $6 \times 5$  min dynamic protocol. PET preprocessing steps for scanner harmonization were identical for all tracers and are described elsewhere (Jagust *et al.*, 2015). Briefly, PET frames were realigned, averaged, reoriented, resliced to a common grid, and smoothed to a common resolution of 8 mm. Further details on PET acquisition and preprocessing in ADNI can be found at <http://adni.loni.usc.edu/methods/documents/>.

For quantitative PET analyses, preprocessed PET images were rigidly co-registered to the closest-in-time corresponding structural  $T_1$  MRI scan using Statistical Parametric Mapping 12 (SPM12; Wellcome Department of Imaging Neuroscience, Institute of Neurology, London, UK).  $T_1$  MRI acquisition protocols and standardized preprocessing steps for scanner harmonization and noise reduction have been described (Jack *et al.*, 2015). The preprocessed  $T_1$  MRI scan was then automatically segmented into grey and white matter tissue segments and high-dimensionally registered to Montreal Neurological Institute (MNI) space using the Computational Anatomy Toolbox (CAT12, <http://dbm.neuro.uni-jena.de/cat/>) in SPM12. Binary grey and white matter masks were created using a threshold of 0.5 over the corresponding tissue probability map in participant space. The inverse of the deformation field resulting from spatial registration was used to propagate regions of interest from MNI to participant space, and the propagated regions of

interest were multiplied by the appropriate binary segment to create the final mask. We generated standardized uptake value ratio (SUVR) images for FBP using a whole cerebellum region of interest (Klunk *et al.*, 2015) as the reference region. Global amyloid- $\beta$  deposition was defined as the mean SUVR in a previously defined cortical composite region of interest (Klunk *et al.*, 2015), and these values were then transformed to centiloid units (Klunk *et al.*, 2015) using equations derived by the ADNI PET Core (<http://adni.loni.usc.edu/data-samples/access-data/>). FBP SUVR images were finally corrected for partial volume effects (PVE) using the Müller-Gärtner method (Gonzalez-Escamilla *et al.*, 2017). For FTP imaging, SUVR maps were created using an inferior cerebellum region of interest (Maass *et al.*, 2017) as the reference region and corrected for PVE using the region-based voxel-wise (RBV) method (Thomas *et al.*, 2011) with a previously defined anatomical parcellation (Baker *et al.*, 2017). To perform voxel-wise analyses, co-registered PET images were spatially normalized to MNI space using the deformation field obtained from spatial normalization of their corresponding MRI scan, and the resulting images were masked with a grey matter mask and smoothed using a 6 mm isotropic filter.

## CSF biomarkers

CSF samples were collected and processed according to previously described protocols (Kang *et al.*, 2015). Concentrations of amyloid- $\beta_{1-42}$  and p-tau181 in CSF were measured by the ADNI Biomarker Core using the Elecsys<sup>®</sup>  $\beta$ -Amyloid(1–42) and the Elecsys<sup>®</sup> Phospho-Tau (181P) CSF immunoassays, respectively, on a cobas e 601 module (Bittner *et al.*, 2016; Hansson *et al.*, 2018). The measuring limits (lower to upper limits) of these assays were 200 to 1700 ng/l for Elecsys<sup>®</sup>  $\beta$ -Amyloid(1–42) and 8 to 120 ng/l for Elecsys<sup>®</sup> Phospho-Tau (181P) assays. Note that absolute p-tau181 concentrations in CSF, as measured by the Elecsys assay, are not comparable with those measured in plasma by the Simoa assay as the assays use different antibodies and calibrators. In our previous study analysing p-tau181 measured in paired plasma and CSF from the same individuals and using the same Simoa assay, we found a mean plasma to CSF p-tau181 ratio of  $\sim 5\%$  (Karikari *et al.*, 2020).

The measuring range of the Elecsys<sup>®</sup>  $\beta$ -Amyloid(1–42) CSF immunoassay beyond the upper technical limit has not been formally established. Therefore, use of values above the upper technical limit, which are provided based on an extrapolation of the calibration curve, is restricted to exploratory research purposes and is excluded for clinical decision-making or for the derivation of medical decision points. In the present study, we included extrapolated values of amyloid- $\beta_{1-42}$  concentrations in all analyses. Longitudinal CSF extractions were performed approximately every 2 years over a median follow-up time of 3.3 years in 410 participants.

## Biomarker cut-off points

To determine amyloid- $\beta$  status (+/–) using amyloid- $\beta$  PET, we used an externally derived cut-off point of 24.4 centiloids that best discriminated between subjects with and without Alzheimer's disease neuropathological changes at autopsy (La Joie *et al.*, 2019). We chose this centiloid-based cut-off point over the traditional ADNI cut-off point of 1.11 SUVR (Landau *et al.*, 2013) as it is derived using a fully neuropathology-defined ground truth and as it provides better cross-cohort comparability and replicability. The cut-off point for CSF amyloid- $\beta_{1-42}$  +/- using the Elecsys assay was also independently determined on the basis of maximal agreement with amyloid- $\beta$  PET (1100 pg/ml) (Hansson *et al.*, 2018; Schindler *et al.*, 2018; Shaw *et al.*, 2018; Willemse *et al.*, 2018). No externally determined cut-off points for p-tau181 markers (CSF and plasma) are currently available, and therefore we derived these cut-off points conservatively by defining them as the 90th percentile of PET amyloid- $\beta$ - cognitively normal individuals ( $n = 190$ ) (Jack *et al.*, 2017), yielding 21.99 pg/ml for plasma p-tau181 and 28.69 pg/ml for CSF p-tau181.

## Statistical analysis

Longitudinal rates of change in plasma p-tau181 levels as well as PET-derived centiloid values and CSF biomarker levels were estimated using linear mixed models with subject-specific intercepts and slopes that predicted biomarker levels over time [ $biomarker \sim time + (time|subject)$ ]. Individual rates of change were derived from these models by summing the fixed and the subject-specific random effects terms and were used for subsequent analyses, as described below.

We first assessed linear associations of baseline plasma p-tau181 levels with cross-sectional and longitudinal estimates of regional amyloid- $\beta$  accumulation as measured by FBP-PET, using voxel-wise linear regressions adjusted for age and sex. Identical models were used to assess associations between longitudinal changes in plasma p-tau181 and increases in voxel-wise FBP-PET signal. To assess a possible disease stage dependency of these associations, all models were computed for the different diagnostic groups separately. Moreover, to further investigate whether plasma p-tau181 reflects continuous amyloid- $\beta$  levels in subjects with or without Alzheimer's disease, we performed analogous analyses stratified by amyloid- $\beta$  status.

Second, we used non-linear smoothing spline regressions to model baseline levels and longitudinal changes in plasma p-tau181 as a function of globally increasing amyloid- $\beta$  pathology, both measured using CSF amyloid- $\beta_{1-42}$  levels and FBP-PET-derived centiloid values. The smoothing parameter was determined via minimization of the mean squared error using a 25-repetition, 10-fold cross-validation procedure. Confidence intervals (95%, CI) were generated using 5000-repetition bootstrap samples. This procedure was also used to describe the dependency between baseline levels and longitudinal change of p-tau181 as measured in plasma and CSF.

Third, we assessed associations of baseline levels and longitudinal changes in plasma p-tau181 with future tau deposition measured on FTP PET 6 years later, using linear voxel-wise regressions adjusted for age, sex, and time difference between FTP scan and blood extraction. Analyses were conducted separately for cognitively normal and cognitively impaired individuals (pooled MCI + Alzheimer's disease dementia due to the low number of patients with Alzheimer's disease dementia), as well as for amyloid- $\beta$ + and amyloid- $\beta$ - individuals.

Finally, we aimed to determine the temporal trajectories of plasma p-tau181 and core Alzheimer's disease biomarkers across the spectrum of sporadic Alzheimer's disease. Under the hypothesis that (i) the studied biomarkers are sufficiently specific for Alzheimer's disease, so that other conditions have no major influence on individual short-term longitudinal changes; and (ii) biomarker levels of individual short-term time series can be placed along a continuous, ordered measure of disease severity, we used a previously developed method for the construction of long-term temporal biomarker trajectories using individual short-term data (Villemagne *et al.*, 2013; Budgeon *et al.*, 2017). Briefly, annualized rates of change were plotted against their corresponding baseline levels and fitted using the above described smoothing spline procedure. Resulting spline curves were finally integrated numerically using Euler's method and anchored to median levels in amyloid- $\beta$ - cognitively normal at  $t = 0$ , resulting in a time axis that reflects the time needed to change from median biomarker levels in the amyloid- $\beta$ - cognitively normal reference group to higher levels.

Statistical analyses were performed using the Statistics and Machine learning toolbox included in MATLAB 2018a (The MathWorks, Inc.). Neuroimaging analyses were performed using SPM12 (multiple regressions, two-sample  $t$ -tests). Results from voxel-wise analyses were assessed using a family-wise error-corrected significance threshold at the cluster level ( $P_{FWE} < 0.001$  or  $P_{FWE} < 0.05$ , depending on sample size) with an initial voxel-wise height threshold of  $P < 0.001$  or  $P < 0.01$ , respectively (see figure legends).

## Data availability

Data used in this study have been made publicly available by the ADNI in the Laboratory of Neuro Imaging (LONI) database.

## Results

### Associations of plasma p-tau181 with regional amyloid- $\beta$ pathology across the Alzheimer's disease clinical spectrum

First, we assessed the cross-sectional associations of plasma p-tau181 with global and regional amyloid- $\beta$  deposition on

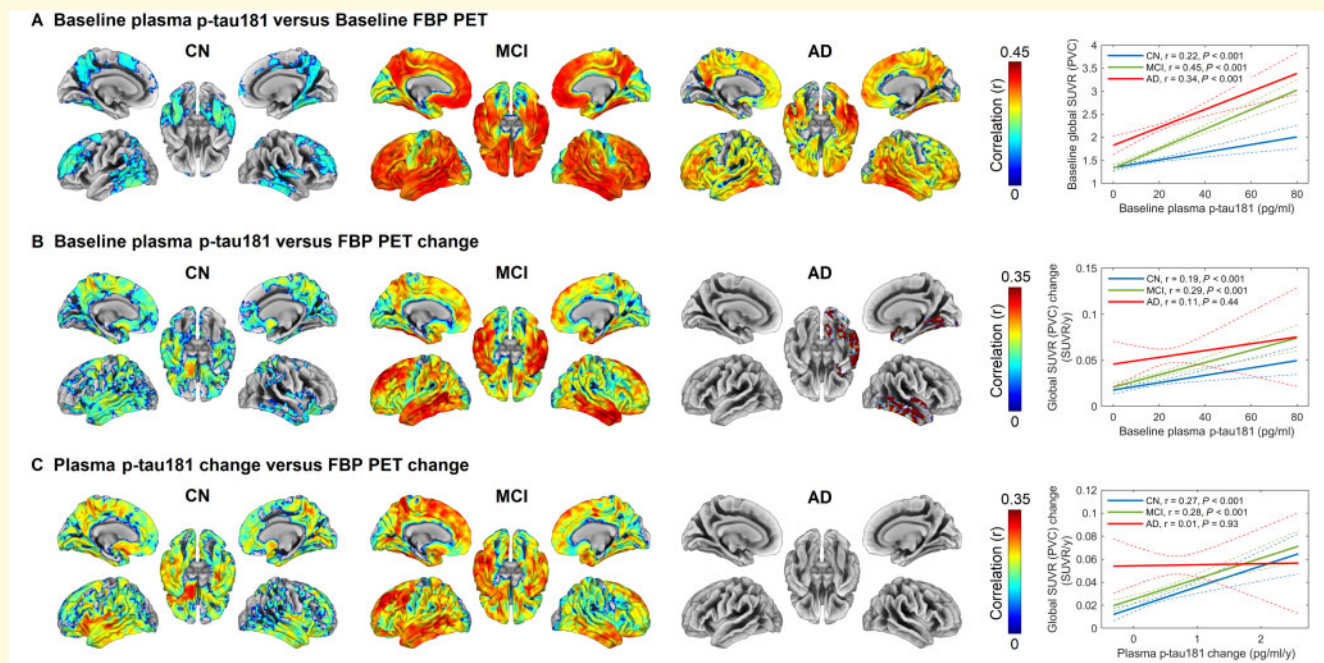


**Figure 1** Regional and global associations of plasma p-tau181 with PET-measured amyloid- $\beta$  deposition and longitudinal accumulation across the clinical spectrum of Alzheimer's disease. Voxel-wise analyses (adjusted for age and sex) assessing regional associations between (A) baseline plasma p-tau181 levels and baseline FBP SUVR, (B) baseline plasma p-tau181 levels and FBP SUVR change, and (C) plasma p-tau181 change and FBP SUVR change. Significant associations in voxel-wise analyses were determined based on a FWE-corrected threshold of  $P < 0.001$  at the cluster level, with initial voxel-level height thresholds of  $P < 0.001$  (A), or  $P < 0.01$  (B and C) (depending on sample size). Colour panels on the right display linear fits and (unadjusted) Pearson correlation coefficients ( $r$ ) of the effects on global measures. Dashed lines in right panels are 95% confidence intervals. In cognitively normal subjects (CN), weak correlations were observed in regions previously described as early amyloid- $\beta$  accumulating regions, while the strongest correlations were observed at the MCI stage where regional associations covered widespread areas involving cortical and subcortical areas known to be involved later in the disease course (see also Supplementary Figs 2 and 3). AD = Alzheimer's disease.

FBP-PET across the clinical spectrum of Alzheimer's disease (Fig. 1A). Baseline levels of plasma p-tau181 associated with amyloid- $\beta$  deposition more strongly in subjects with MCI and Alzheimer's disease dementia, while associations were markedly weaker among cognitively normal participants. The observed association patterns in patients with MCI and Alzheimer's disease dementia covered widespread areas of the cortex and expanded subcortically to the striatum (Supplementary Fig. 2). In contrast, the weaker associations observed in cognitively normal subjects were restricted to the precuneus and to temporal and superior-frontal areas, and did not involve subcortical structures, suggesting that plasma p-tau181 associates more strongly with amyloid- $\beta$  pathology when amyloid- $\beta$  deposits are present in widespread areas of the brain. Results were similar when using global composite PET imaging measures of amyloid- $\beta$  pathology (Fig. 1A,  $r = 0.18$  in cognitively normal,  $r = 0.41$  in MCI, and  $r = 0.35$  in Alzheimer's disease,  $P < 0.001$  for all age and sex-adjusted associations). We then investigated the correlations of baseline and change measures of plasma p-tau181 with longitudinal amyloid- $\beta$  accumulation in serial FBP-PET (Fig. 1B and C). The strongest associations were again observed in MCI participants, followed by cognitively

normal subjects. Only marginal and statistically non-significant associations were found for patients with Alzheimer's disease dementia, which, however, also had a much smaller sample size. Similar to the cross-sectional findings, regional association patterns in cognitively normal and MCI individuals revealed that both elevated baseline levels and longitudinal increases of plasma p-tau181 were associated with longitudinal amyloid- $\beta$  accumulation in large areas of the temporal, frontal, and parietal cortices, as well as in the striatum (Supplementary Fig. 3), which suggests a stronger association of plasma p-tau181 with amyloid- $\beta$  in advanced stages of brain amyloidosis. Associations with global longitudinal amyloid- $\beta$  accumulation were statistically significant for cognitively normal ( $r = 0.17, P = 0.006$  for baseline plasma p-tau181,  $r = 0.22, P < 0.001$  for change in plasma p-tau181) and MCI ( $r = 0.27$  for baseline,  $r = 0.26$  for change,  $P < 0.001$  for both) but not for Alzheimer's disease dementia subjects ( $r = 0.23, P = 0.12$  for baseline and  $r = 0.03, P = 0.79$  for change). In analyses stratified by amyloid- $\beta$  status, the previous associations were only observed among amyloid- $\beta$ + subjects, independent of cognitive impairment, which suggests that plasma p-tau181 levels reflect a progressive pathological state rather than continuous

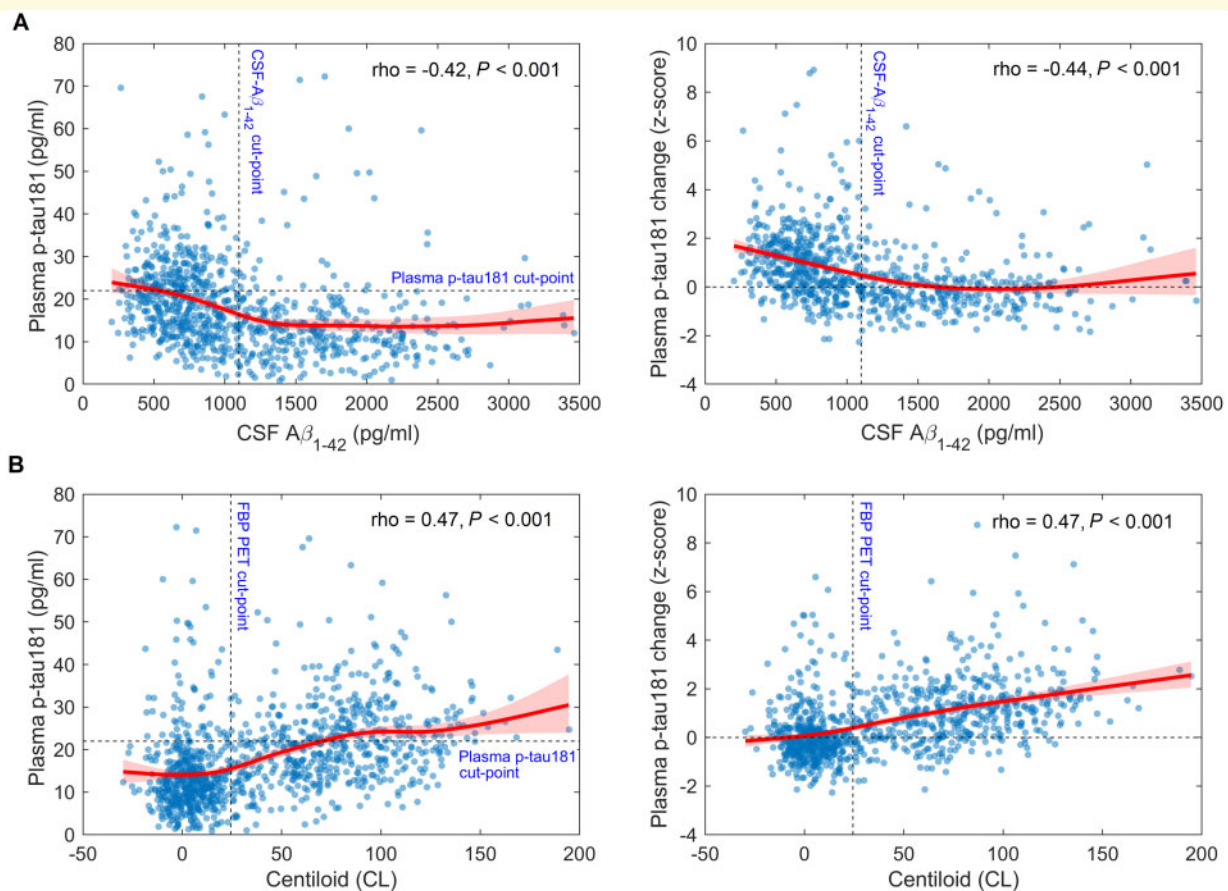


**Figure 2** Baseline and longitudinal associations of plasma p-tau181 with imaging and CSF biomarkers of global amyloid- $\beta$  pathology. Smoothing splines describing the statistical dependence of baseline levels of plasma p-tau181 (left) and longitudinal change in plasma p-tau181 (right) on (A) CSF amyloid- $\beta_{1-42}$  levels and (B) global centiloids. Spearman's rank correlation was used to quantify the monotonic correlation between these measures. Shaded areas are 95% CI for the fit. Dashed lines represent cut-off points for abnormality for the studied biomarkers. Earliest increases in plasma p-tau181 appeared shortly before amyloid- $\beta$  markers reached abnormal levels, and changes accelerated as the severity of global amyloid- $\beta$  pathology increased. Plasma p-tau181 reached abnormal levels only after amyloid- $\beta$  biomarkers reached relatively advanced abnormality levels (PET centiloid = 70 pg/ml and CSF amyloid- $\beta_{1-42}$  = 540 pg/ml, left).

amyloid- $\beta$  levels in subjects without Alzheimer's disease (Supplementary Fig. 4).

## Plasma p-tau181 dynamic changes and amyloid- $\beta$ pathology

Using smoothing splines, we observed that earliest elevations in baseline plasma p-tau181 levels as a function of global amyloid- $\beta$  pathology occurred even before FBP-PET and CSF amyloid- $\beta_{1-42}$  reached their respective abnormality thresholds (Fig. 2A and B), demonstrating consistent increases as amyloid- $\beta$  pathology progresses. This cross-sectional result was confirmed when analysing the dependence of plasma p-tau181 change rates on amyloid- $\beta$  biomarker levels: a small but significant (i.e. 95% CI, not including  $z = 0$ ) deviation from normative levels in the standardized change rate was observed at subthreshold levels for both FBP-PET and CSF amyloid- $\beta_{1-42}$  (Fig. 2A and B) and this change continued accelerating as the severity of amyloid- $\beta$

pathology increased. The cut-off point for abnormal levels of plasma p-tau181, as defined above, was reached at relatively advanced levels of global amyloid- $\beta$  pathology (centiloid = 70 and CSF amyloid- $\beta_{1-42}$  = 540 pg/ml, estimated by intersecting the spline curve with the p-tau181 cut-off point line), confirming our previous regional neuroimaging analyses. Similarly, analyses stratified by cognitive status (cognitively normal versus cognitively impaired) further confirmed our previous regional analyses, yielding stronger associations between plasma p-tau181 and amyloid- $\beta$  markers among cognitively impaired individuals (Supplementary Fig. 5). Again, the observed associations were only present among amyloid- $\beta$ + subjects (Supplementary Fig. 6).

## Associations between p-tau181 levels in plasma and in CSF

Smoothing splines demonstrated that cross-sectional p-tau181 levels in plasma and in CSF were correlated up to

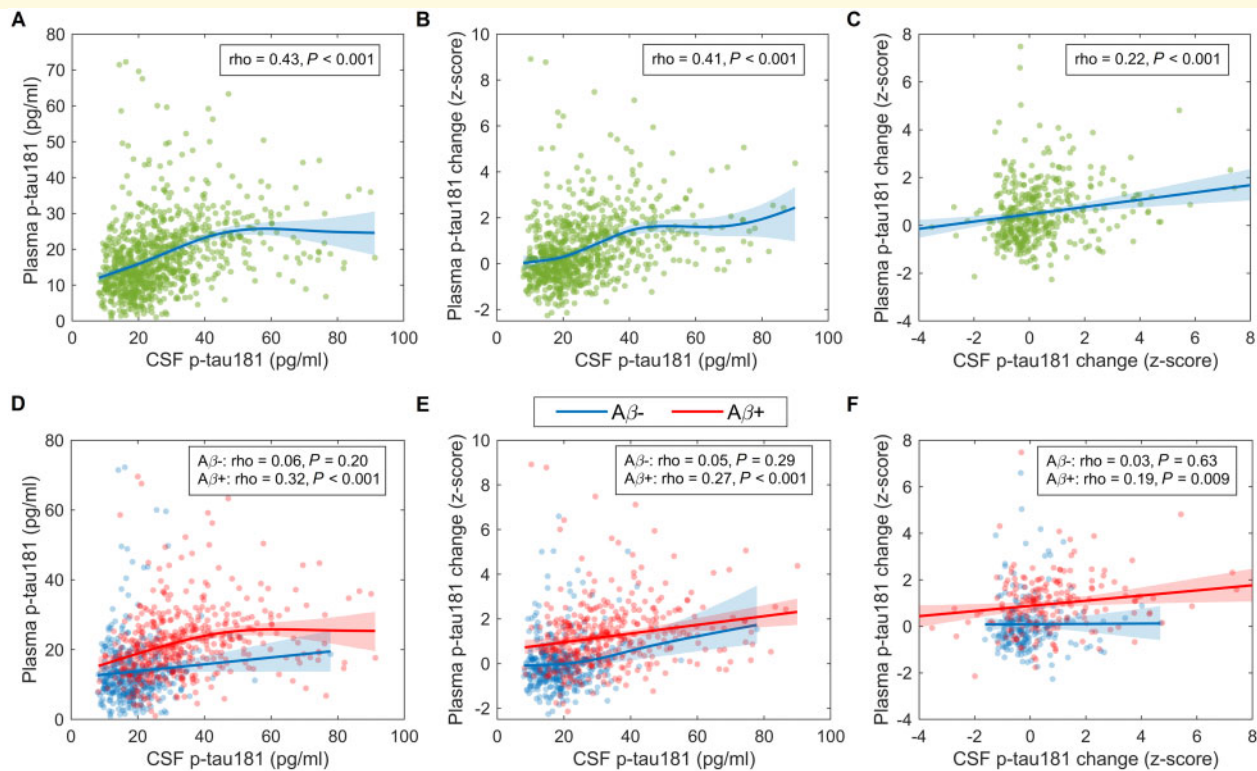


**Figure 3** Baseline and longitudinal associations between plasma p-tau181 and CSF p-tau181. Smoothing splines describing the statistical dependence of baseline levels of plasma p-tau181 (A) and plasma p-tau181 change (B) on CSF p-tau181 levels, as well as plasma p-tau181 change versus CSF p-tau181 change (C). (D–F) Results from the same analyses stratified by amyloid- $\beta$  status. Z-scores were computed using amyloid- $\beta^-$  cognitively normal levels as the reference. Shaded areas are 95% CI for the fit. Spearman's rank correlation was used to quantify the monotonic correlation between these measures. Changes of p-tau181 in plasma and CSF followed a linear trend approximately anchored at the origin, indicating that these two markers follow similar dynamics. (D–F) Panels show that this association was statistically significant only among amyloid- $\beta^+$  subjects.

relatively high levels of CSF p-tau181 ( $\sim 50$  pg/ml) (Fig. 3A). Moreover, longitudinal increases in plasma p-tau181 were found to accelerate with increasing baseline CSF p-tau181 levels (Fig. 3B). The p-tau181 change rates in plasma and in CSF followed a linear trend approximately anchored at z-scores (0,0), indicating that these two measures follow similar dynamics (Fig. 3C). Analyses stratified by amyloid- $\beta$  status demonstrated that these associations were mainly driven by amyloid- $\beta^+$  individuals (Fig. 3D–F). In contrast, cognitive status did not influence the relationship between p-tau181 in plasma and in CSF among amyloid- $\beta^+$  subjects (Supplementary Fig. 7).

### Associations between plasma p-tau181 and regional tau deposition 6 years later

We then investigated whether baseline and change measures of plasma p-tau181 correlated with the severity of PET-measured tau pathology 6 years later (Fig. 4). In cognitively normal subjects, baseline plasma p-tau181 correlated with future tau pathology in brain regions mainly restricted to the medial temporal and posterior cingulate cortex (Fig. 4A).

In cognitively impaired individuals, associations were stronger and statistically significant in broader areas of the cortex, particularly in lateral temporo-parietal cortical areas. Compared to baseline measures, longitudinal increase in plasma p-tau181 was even stronger associated with brain tau pathology 6 years later, particularly in cognitively normal individuals (Fig. 4B). Thus, significant associations in both cognitively normal and cognitively impaired individuals were observed across a pronounced temporoparietal cortical pattern that closely resembled the stereotypical spatial pattern of NFT aggregation in Alzheimer's disease. When repeating these analyses stratified by amyloid- $\beta$  status (and after adjusting for age, sex, time lag, and cognitive status), plasma p-tau181 baseline levels and longitudinal change were associated with future tau aggregation only among amyloid- $\beta^+$  subjects (Fig. 5).

### Temporal trajectories of plasma p-tau181 in comparison to established Alzheimer's disease biomarkers

We finally determined the temporal trajectory followed by plasma p-tau181 levels and compared it to the trajectories



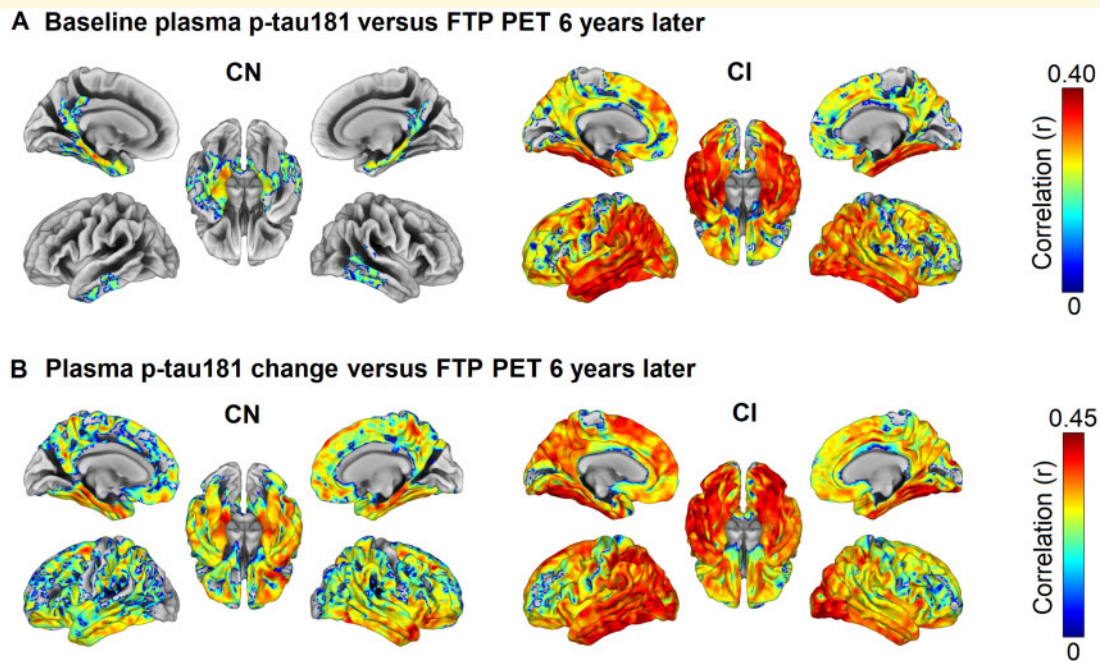


**Figure 4 Associations of plasma p-tau181 baseline levels and longitudinal increase with regional tau aggregation 6 years later, according to cognitive status.** Regional associations (adjusted for age, sex, and time difference between blood sampling and PET scanning) of (A) baseline plasma p-tau181 levels and (B) longitudinal plasma p-tau181 change with voxel-wise FTP SUVR 6 years later. Significant associations in voxel-wise analyses were determined based on a FWE-corrected threshold of  $P < 0.001$  at the cluster level after applying a voxel-level threshold of  $P < 0.01$ . Baseline plasma p-tau181 and, more pronounced, longitudinal change were associated with widespread tau aggregation 6 years later, following the characteristic temporoparietal pattern of progressing neurofibrillary tangle pathology in Alzheimer's disease. CI = cognitively impaired; CN = cognitively normal.

of established PET and CSF Alzheimer's disease biomarkers. Smoothing splines demonstrated that both PET and CSF-based amyloid- $\beta$  biomarker rates of change showed an inverted-U shaped dependence on baseline values (Fig. 6A), indicating that change rates for these markers decelerate for highly abnormal baseline levels. A similar relationship was observed for plasma p-tau181; however, the relatively wide confidence interval at higher p-tau181 levels with less available data-points could in fact indicate monotonic growth (Fig. 6A). Similarly, CSF p-tau181 change increased in a linear manner over the entire range of baseline values. Smoothing splines in Fig. 6A were integrated and anchored at median levels of amyloid- $\beta$ —cognitively normal to derive comparative temporal trajectories of plasma p-tau181, FBP-PET, and CSF biomarkers (Fig. 6B). Plasma p-tau181 reached abnormal levels after 23.2 (95% CI: 22.0 to 22.4) years (Fig. 6B), significantly later than CSF amyloid- $\beta_{1-42}$  (16.7 years, difference  $-6.5$ , 95% CI:  $-8.6$  to  $-4.1$ ) and FBP-PET (17.5 years, difference  $-5.7$  years, 95% CI:  $-7.8$  to  $-3.2$ ) (Fig. 6B). Plasma p-tau181 and CSF p-tau181 followed very similar trajectories, the latter reaching abnormal levels 2 years after plasma p-tau181, although this difference was not statistically significant (95% CI:  $-0.2$  to 4.65). For reference, we show within-participant trajectories

(spaghetti plots) of plasma p-tau181 accumulation as a function of time from baseline (Supplementary Fig. 8).

## Discussion

In the present prospective longitudinal study, we provide a detailed description of the temporal dynamics of plasma p-tau181, from the earliest manifestations of Alzheimer's disease pathology in cognitively normal individuals to the dementia stage. Our findings indicate that (i) established amyloid- $\beta$  pathology associates with dynamic changes of p-tau181 in blood; (ii) elevated levels of plasma p-tau181 associate with elevated tau-PET signal 6 years later, with a spatial distribution that closely matches the typical predilection sites of NFT pathology in Alzheimer's disease; and (iii) p-tau181 in blood largely reflects the dynamics of p-tau181 in CSF. Taken together, these results suggest that plasma p-tau181 reflects features of tau pathology that are intimately related to fibrillar amyloid- $\beta$  pathology and that might be predictive of downstream aggregation of tau fibrils several years before established NFT pathology. Our findings thus extend prior results from three recent cross-sectional studies (Janelidze *et al.*, 2020; Karikari *et al.*, 2020; Thijssen *et al.*, 2020) and from a study in familial Alzheimer's disease (O'Connor *et al.*, 2020), providing a

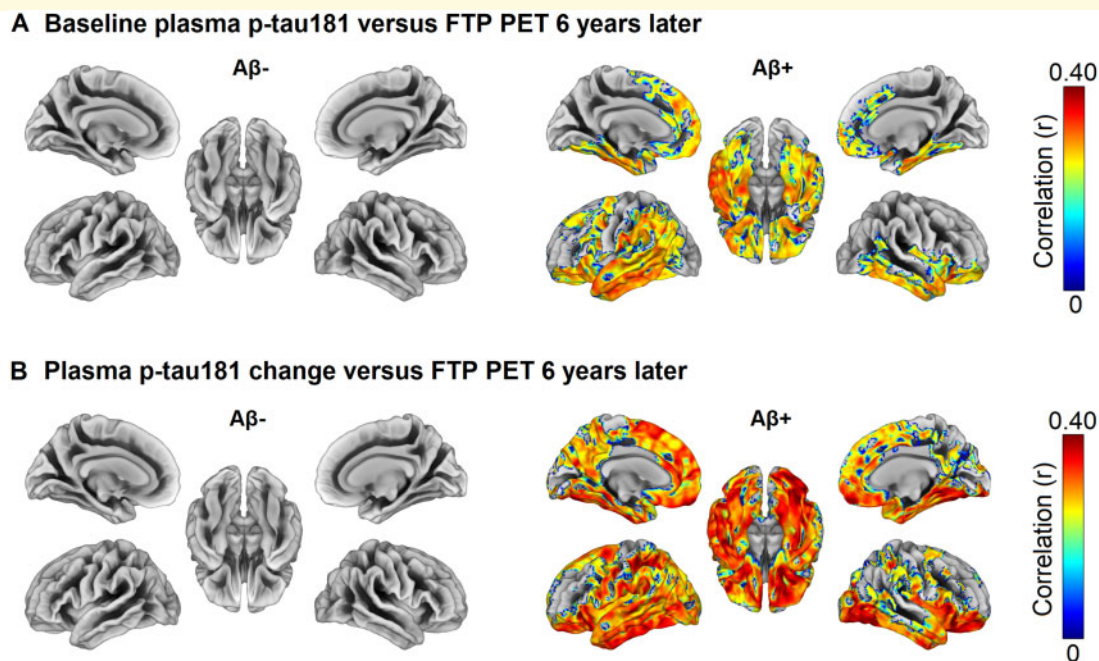


**Figure 5 Associations of plasma p-tau181 baseline levels and longitudinal increase with regional tau aggregation 6 years later, stratified by amyloid- $\beta$  status.** Regional associations (adjusted for age, sex, cognitive status, and time difference between blood sampling and PET scanning) of (A) baseline plasma p-tau181 levels and (B) longitudinal plasma p-tau181 change with voxel-wise FTP SUVR 6 years later. Significant associations in voxel-wise analyses were determined based on a FWE-corrected threshold of  $P < 0.05$  at the cluster level after applying a voxel-level threshold of  $P < 0.01$ . Baseline plasma p-tau181 and longitudinal change were associated with widespread tau aggregation 6 years later only among amyloid- $\beta$ + subjects.

more comprehensive picture of the pathological processes reflected by this ultrasensitive measure of p-tau181 in blood. Moreover, by analysing longitudinal changes on multimodal biomarker data, we determined, for the first time, the precise sequence of pathological events that accompany the natural course of plasma p-tau181 changes across the spectrum of Alzheimer's disease.

First, studies of the novel plasma p-tau181 assays could demonstrate a good correspondence of plasma p-tau181 levels with a positive amyloid- $\beta$  and tau status as measured with PET (Janelidze *et al.*, 2020; Karikari *et al.*, 2020; Thijssen *et al.*, 2020). However, the strength of the associations with PET-measured amyloid- $\beta$  and tau pathologies was not consistent across studies, with two studies showing stronger associations with amyloid- $\beta$  (Karikari *et al.*, 2020; Thijssen *et al.*, 2020) and the third with tau (Janelidze *et al.*, 2020), leaving unclear the specific pathological process best reflected by plasma p-tau181. Moreover, these studies were limited by their cross-sectional design and could not provide direct insights into the temporal dynamics of plasma p-tau181 changes in relation to established PET and CSF-based biomarkers of Alzheimer's disease pathology. Therefore, the ability of plasma p-tau181 to detect early pathological features of the disease was not clear.

A first key finding of our longitudinal study describes that the earliest dynamic changes in plasma p-tau181 levels occurred even before PET and CSF biomarkers for amyloid-

$\beta$  pathology reached abnormal levels (Fig. 2). Moreover, the dynamics of plasma p-tau181 increases accelerated as the severity of amyloid- $\beta$  pathology increased, reaching abnormal levels  $\sim 5$  years after established amyloid- $\beta$  pathology (Fig. 6). Consistent with these findings, we found that the associations of plasma p-tau181 with regional amyloid- $\beta$  deposition as measured with FBP-PET were stronger when amyloid- $\beta$  deposits had significantly spread throughout the cortex (Fig. 1). Further, plasma p-tau181 changes were associated with longitudinal amyloid- $\beta$  accumulation in several cortical and subcortical areas that have been previously identified as late-accumulating areas in the disease course (Thal *et al.*, 2002; Grothe *et al.*, 2017; Palmqvist *et al.*, 2017; Hanseeuw *et al.*, 2018). Plasma p-tau181 associations with amyloid- $\beta$  accumulation were marginal among patients with Alzheimer's disease dementia, suggesting amyloid- $\beta$  saturation effects at this stage (Jack *et al.*, 2013). Overall, these results suggest that early amyloid- $\beta$  pathology associates with tau dysregulation and subsequent release of soluble p-tau181 in blood, which escalates at more advanced amyloid- $\beta$  stages. This is in line with previous *in vitro* (De Felice *et al.*, 2008; Jin *et al.*, 2011) and *in vivo* animal findings (Zheng *et al.*, 2002; Shin *et al.*, 2007), as well as results from recent reports on p-tau181 in CSF (Palmqvist *et al.*, 2019; Mattsson-Carlgen *et al.*, 2020).

A second key finding of our study revealed that baseline plasma p-tau181 levels and, more pronounced, longitudinal

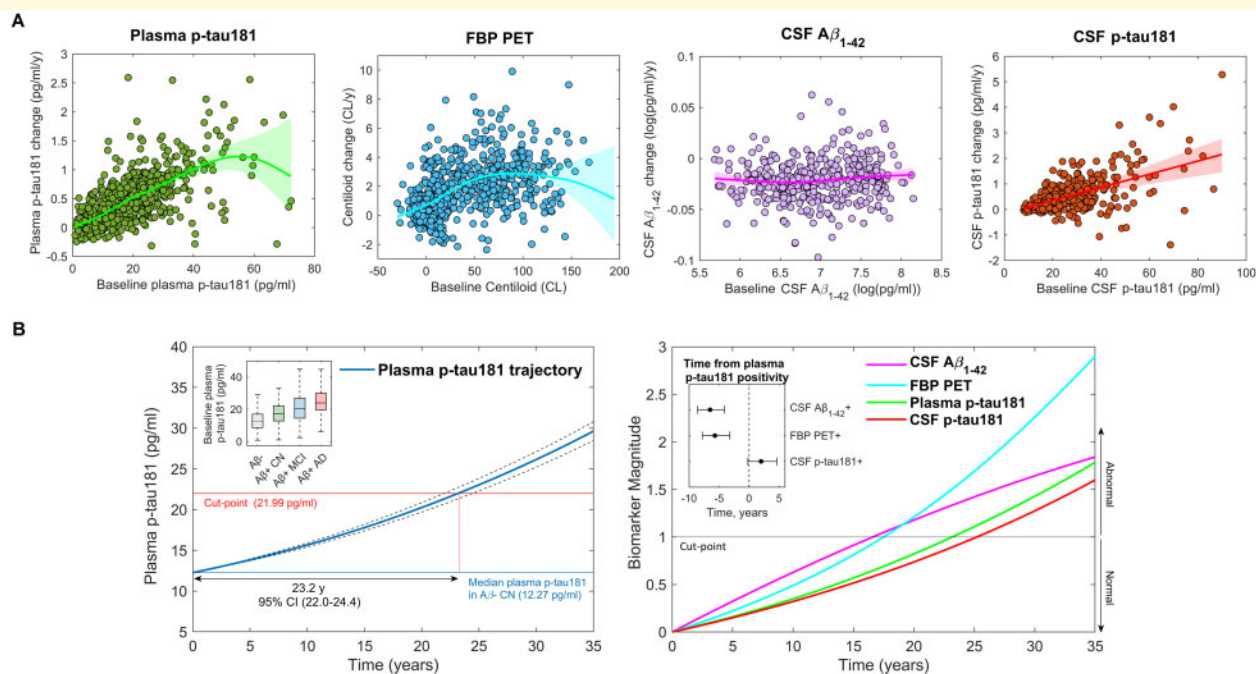


**Figure 6** The natural time course of plasma p-tau181 in Alzheimer's disease. **(A)** Smoothing splines describing the dependence of biomarker rate of change on baseline levels of the respective biomarker. Logarithmic transformation of CSF amyloid- $\beta_{1-42}$  levels was performed in order to improve residual normality in linear mixed models and facilitate the spline fit. **(B)** *Left*: Time course of plasma p-tau181, estimated using individual longitudinal data. The curve is anchored at median plasma p-tau181 levels in cognitively normal amyloid- $\beta^-$  individuals, thus describing the temporal trajectory from non-pathological to abnormal levels. The *inset* shows a box plot representing biomarker levels for amyloid- $\beta^-$  and amyloid- $\beta^+$  subjects at different stages of Alzheimer's disease. *Right*: Combined temporal trajectories of plasma p-tau181, amyloid- $\beta$  PET and CSF biomarkers. To represent all trajectories on the same scale, curves were anchored to median levels in cognitively normal amyloid- $\beta^-$  subjects, transformed to z-scores using mean cognitively normal amyloid- $\beta^-$  levels as reference, and scaled to the corresponding cut-off point z-score (Villemagne *et al.*, 2013). The *inset* demonstrates the time lag between time points where plasma p-tau181 and other biomarkers reach abnormal levels. Plasma p-tau181 reached abnormal levels  $\sim 5.7$  years after amyloid- $\beta$  PET and 6.5 years after CSF amyloid- $\beta_{1-42}$ , following similar dynamics as CSF p-tau181, which reached abnormal levels 2.0 years after plasma p-tau181 (not statistically significant).

plasma p-tau181 increases, were associated with PET-measured tau aggregation 6 years later (Fig. 4), suggesting that the progressive accumulation of soluble p-tau181 might be a marker of tau fibril aggregation. Interestingly, baseline plasma p-tau181 levels even predicted spatially restricted tau aggregation in cognitively normal individuals, coinciding with typical limbic predilection sites of initial NFT formation (Braak *et al.*, 2006; Brier *et al.*, 2016; Johnson *et al.*, 2016; Schöll *et al.*, 2016; Bejanin *et al.*, 2017; Hanseeuw *et al.*, 2019). By contrast, dynamic increases in plasma p-tau181 levels correlated with NFT pathology in widespread cortical areas exceeding the medial temporal lobe, following a typical temporoparietal distribution pattern characteristic for NFT deposition associated with advanced Braak stages (Braak *et al.*, 2006; Schöll *et al.*, 2019). These findings extend results from previous studies showing cross-sectional associations between elevations in plasma p-tau181 and widespread PET-measured NFT deposition (Janelidze *et al.*, 2020; Karikari *et al.*, 2020; Thijssen *et al.*, 2020), demonstrating the potential of plasma p-tau181 as an accessible measure of pathological features of Alzheimer's disease that relate more closely with clinical decline (Brier *et al.*, 2016;

Bejanin *et al.*, 2017; Hanseeuw *et al.*, 2019; Janelidze *et al.*, 2020; Karikari *et al.*, 2020).

In line with recent cross-sectional studies, we found moderate associations between p-tau181 levels in blood and CSF (Janelidze *et al.*, 2020; Karikari *et al.*, 2020). Further, we extended these previous observations by noting that p-tau181 in blood and CSF followed similar longitudinal dynamics (Figs 3C and 6B), suggesting that elevations of plasma p-tau181 in blood and CSF reflect comparable underlying pathological processes. Although not statistically significant, we observed that plasma p-tau181 reached the cut-off point for abnormality 2 years before CSF p-tau181. This finding is of interest taking into account that p-tau181 release into blood is believed to be downstream to that into CSF. However, two factors may explain this statistically non-significant difference. First, the relative time lag derived from Fig. 6B is cut-off point-dependent (see also limitations below), therefore the small time difference until abnormality levels are reached in plasma and CSF-derived p-tau181 levels may relate to non-equivalent cut-off point estimates for the two markers. Second, the plasma and CSF p-tau181 assays used in the present study possess different properties.

Although both target p-tau181, the tau species measured by each assay are different (N-terminal phosphorylated tau in the plasma assay compared with mid-region fragments in the CSF assay). Therefore, the observed difference could theoretically also relate to a difference in detectability of different tau species. However, this is currently purely speculative and would require more focused research. Similarly, differences in diagnostic performance and predictive power between these two p-tau181 markers remain to be elucidated and are currently the focus of an ongoing investigation by our group.

Our findings have clear implications for the use of plasma p-tau181 as a diagnostic test for early Alzheimer's disease. First, the observation that prominent changes in plasma p-tau181 coincide with the presence of established amyloid- $\beta$  pathology indicates that these elevations are highly specific for Alzheimer's disease neuropathological changes. Second, plasma p-tau181 levels reached abnormality thresholds  $\sim$ 5 years after manifest brain amyloidosis as detected by amyloid- $\beta$  PET or CSF amyloid- $\beta_{1-42}$ . Since overt neurodegeneration and cognitive decline occur many years (even decades) after amyloid- $\beta$  positivity is reached (Villemagne *et al.*, 2013; Baek *et al.*, 2020), this indicates that, from a clinical perspective, plasma p-tau181 can be regarded as an early biomarker for Alzheimer's disease. Third, the ability of plasma p-tau181 and its longitudinal accumulation to forecast widespread tau tangle deposition suggests that this marker may be suitable to track Alzheimer's disease progression up to advanced disease stages that strongly associate with cognitive decline.

The results presented in this study may also have relevant implications for disease-modifying treatment trials of Alzheimer's disease. One of the main potential applications of plasma p-tau181 is its use as a screening tool prior to amyloid- $\beta$  or tau PET confirmatory scans, likely resulting in highly reduced costs (Jack, 2020). In this regard, our findings indicate that, although coinciding with an early clinical stage, elevated plasma p-tau181 levels associate with a disease stage of several years of pathological disease progression that likely reflects an established disruption of tau metabolism leading to NFT formation. Thus, patient selection based on plasma p-tau181 may be detrimental for trials that target earlier features of the disease such as early amyloid- $\beta$  pathology (Sperling *et al.*, 2014). Nevertheless, the fact that plasma p-tau181 correlated with the severity of tau pathology several years later suggests that this marker may be particularly useful for screening participants in clinical trials targeting tau pathology (Congdon and Sigurdsson, 2018). Future studies are warranted to elucidate the power of plasma p-tau181 as an estimator of target engagement in tau trials.

Strengths of our study include using data from a large, prospective cohort with multimodal biomarker data to explore the associations between plasma p-tau181 and established biomarkers of different aspects of Alzheimer's disease pathology in a relatively unbiased manner. Second, we used a longitudinal design with comparably comprehensive and

long follow-up data that allowed the derivation of a robust estimate of the temporal trajectory of plasma p-tau181 changes in direct comparison with those of established Alzheimer's disease biomarkers. Limitations include: (i) tau PET was not acquired concurrently to plasma p-tau181 and therefore we could only assess associations between plasma p-tau181 and regional tau deposition 6 years later, whereas the baseline levels of tau deposition remain unknown. Effects of plasma p-tau181 changes on regional tau accumulation rates will have to be studied in more detail using serial PET data; (ii) the estimated time point at which plasma p-tau181 levels reach abnormality in the temporal trajectory models ( $\sim$ 5 years from amyloid- $\beta$  positivity) obviously depends on the used cut-off for denoting abnormality. Since no universally accepted cut-off points for plasma or CSF p-tau181 levels are currently available in the literature, we used a commonly used method for cut-off derivation in the biomarker field based on the distribution in a non-pathological (in this case amyloid- $\beta$ -) control population (Jack *et al.*, 2017). While more research on optimal plasma p-tau181 cut-offs is necessary, we note that this method yielded a cut-off for CSF p-tau181 that was very similar to previously proposed cut-offs for this biomarker (Blennow *et al.*, 2019; Mattsson *et al.*, 2019; Meyer *et al.*, 2020). Moreover, the conservative nature of our approach ensures maximal specificity, which is the most desirable feature of this biomarker from a clinical perspective; (iii) the derivation of biomarker temporal trajectories relies on our selected modelling approach; other modelling strategies might result in differences in time to events and curve shape. However, our findings were relatively consistent with those obtained in other biomarker modelling studies (Jack *et al.*, 2013; Villemagne *et al.*, 2013; Budgeon *et al.*, 2017; Baek *et al.*, 2020); (iv) high dropout rates in the Alzheimer's disease dementia group limited our statistical power to detect regional associations with longitudinal amyloid- $\beta$  pathology. However, several previous studies have indicated little dynamic amyloid- $\beta$  changes at this disease stage (Villemagne *et al.*, 2011, 2013; Jack *et al.*, 2013); (v) only four subjects with Alzheimer's disease dementia were scanned using tau PET, leaving it unclear how plasma p-tau181 specifically associates with tau pathology in this advanced disease stage; and (vi) the ADNI is a highly preselected cohort, which, for example, did not include participants with significant vascular pathologies. Our findings can thus not easily be extrapolated to the population at large, and possible effects of vascular pathology (Graff-Radford *et al.*, 2019; Caballero *et al.*, 2020; Moscoso *et al.*, 2020) and other common comorbidities on amyloid- $\beta$  and plasma p-tau181 levels remain to be studied in less selected cohorts.

In conclusion, we provide a detailed picture of the temporal trajectory followed by plasma p-tau181 in the context of established Alzheimer's disease biomarkers, in which elevations of plasma p-tau181 are tightly linked to established amyloid- $\beta$  pathology. Moreover, dynamic changes of plasma p-tau181 closely resembled those of CSF p-tau181, suggesting that both markers reflect similar underlying pathological

processes. Finally, plasma p-tau181 levels associated with advanced regional tau deposition, as detected by PET several years after the blood test. Together, these findings strongly support the use of this novel blood biomarker as a diagnostic and screening tool for Alzheimer's disease.

## Funding

M.J.G. is supported by the “Miguel Servet” program [CP19/00031] of the Spanish Instituto de Salud Carlos III (ISCIII-FEDER). T.K.K. holds a research fellowship from the Brightfocus Foundation (#A2020812F), and is further supported by the Swedish Alzheimer Foundation (Alzheimerfonden; #AF-930627), the Swedish Brain Foundation (Hjärnfonden; #FO2020-0240), the Swedish Dementia Foundation (Demensförbundet), the Agneta Prytz-Folkes & Gösta Folkes Foundation (#2020-00124), the Aina (Ann) Wallströms and Mary-Ann Sjöbloms Foundation, the Anna Lisa and Brother Björnsson's Foundation, Gamla Tjänarinnor, and the Gun and Bertil Stohnes Foundation. A.S. is supported by the Paulo Foundation and the Orion Research Foundation. M.S.C. received funding from the European Union's Horizon 2020 Research and Innovation Program under the Marie Skłodowska-Curie action grant agreement No 752310, and currently receives funding from Instituto de Salud Carlos III (PI19/00155) and from the Spanish Ministry of Science, Innovation and Universities (Juan de la Cierva Programme grant IJC2018-037478-I). H.Z. is a Wallenberg Scholar supported by grants from the Swedish Research Council (#2018-02532), the European Research Council (#681712), Swedish State Support for Clinical Research (#ALFGBG-720931), the Alzheimer Drug Discovery Foundation (ADDF), USA (#201809-2016862), and the UK Dementia Research Institute at UCL. K.B. is supported by the Swedish Research Council (#2017-00915), the Alzheimer Drug Discovery Foundation (ADDF), USA (#RDAPB-201809-2016615), the Swedish Alzheimer Foundation (#AF-742881), Hjärnfonden, Sweden (#FO2017-0243), the Swedish state under the agreement between the Swedish government and the County Councils, the ALF-agreement (#ALFGBG-715986), and European Union Joint Program for Neurodegenerative Disorders (JPND2019-466-236). M.S. is supported by the Knut and Alice Wallenberg Foundation (Wallenberg Centre for Molecular and Translational Medicine; KAW 2014.0363), the Swedish Research Council (#2017-02869), the Swedish state under the agreement between the Swedish government and the County Councils, the ALF-agreement (#ALFGBG-813971), and the Swedish Alzheimer Foundation (#AF-740191). Data collection and sharing for this project was funded by the Alzheimer's Disease Neuroimaging Initiative (ADNI) (National Institutes of Health Grant U01 AG024904) and DOD ADNI (Department of Defense award number W81XWH-12-2-0012). ADNI is funded by the National Institute on Aging, the National Institute of Biomedical

Imaging and Bioengineering, and through generous contributions from the following: AbbVie, Alzheimer's Association; Alzheimer's Drug Discovery Foundation; Araclon Biotech; BioClinica, Inc.; Biogen; Bristol-Myers Squibb Company; CereSpir, Inc.; Cogstate; Eisai Inc.; Elan Pharmaceuticals, Inc.; Eli Lilly and Company; EuroImmun; F. Hoffmann-La Roche Ltd and its affiliated company Genentech, Inc.; Fujirebio; GE Healthcare; IXICO Ltd.; Janssen Alzheimer Immunotherapy Research & Development, LLC.; Johnson & Johnson Pharmaceutical Research & Development LLC.; Lumosity; Lundbeck; Merck & Co., Inc.; Meso Scale Diagnostics, LLC.; NeuroRx Research; Neurotrack Technologies; Novartis Pharmaceuticals Corporation; Pfizer Inc.; Piramal Imaging; Servier; Takeda Pharmaceutical Company; and Transition Therapeutics. The Canadian Institutes of Health Research is providing funds to support ADNI clinical sites in Canada. Private sector contributions are facilitated by the Foundation for the National Institutes of Health ([www.fnih.org](http://www.fnih.org)). The grantee organization is the Northern California Institute for Research and Education, and the study is coordinated by the Alzheimer's Therapeutic Research Institute at the University of Southern California. ADNI data are disseminated by the Laboratory for Neuro Imaging at the University of Southern California.

## Competing interests

H.Z. has served at scientific advisory boards for Denali, Roche Diagnostics, Wave, Samumed, Siemens Healthineers, Pinteon Therapeutics and CogRx, has given lectures in symposia sponsored by Fujirebio, Alzecure and Biogen, and is a co-founder of Brain Biomarker Solutions in Gothenburg AB (BBS), which is a part of the GU Ventures Incubator Program (outside submitted work). K.B. has served as a consultant, at advisory boards, or at data monitoring committees for Abcam, Axon, Biogen, JOMDD/Shimadzu. Julius Clinical, Lilly, MagQu, Novartis, Roche Diagnostics, and Siemens Healthineers, and is a co-founder of Brain Biomarker Solutions in Gothenburg AB (BBS), which is a part of the GU Ventures Incubator Program. M.S. has served on a scientific advisory board for Servier Pharmaceuticals (outside submitted work). A.M., M.J.G., N.J.A., T.K.K., J.L.R., A.S., and M.S.C. report no competing interests.

## Supplementary material

Supplementary material is available at *Brain* online.

## References

Ashton NJ, Hye A, Rajkumar AP, Leuzy A, Snowden S, Suarez-Calvet M, et al. An update on blood-based biomarkers for non-Alzheimer neurodegenerative disorders. *Nat Rev Neurol* 2020; 16: 265–84.

- Ashton NJ, Nevado-Holgado AJ, Barber IS, Lynham S, Gupta V, Chatterjee P, et al. A plasma protein classifier for predicting amyloid burden for preclinical Alzheimer's disease. *Sci Adv* 2019; 5: eaau7220.
- Baek MS, Cho H, Lee HS, Choi JY, Lee JH, Ryu YH, et al. Temporal trajectories of in vivo tau and amyloid-beta accumulation in Alzheimer's disease. *Eur J Nucl Med Mol Imaging* 2020; 47: 2879–86.
- Baker SL, Maass A, Jagust WJ. Considerations and code for partial volume correcting [(18)F]-AV-1451 tau PET data. *Data Brief* 2017; 15: 648–57.
- Barthelemy NR, Horie K, Sato C, Bateman RJ. Blood plasma phosphorylated-tau isoforms track CNS change in Alzheimer's disease. *J Exp Med* 2020; 217: e20200861.
- Bejanin A, Schonhaut DR, La Joie R, Kramer JH, Baker SL, Sosa N, et al. Tau pathology and neurodegeneration contribute to cognitive impairment in Alzheimer's disease. *Brain* 2017; 140: 3286–300.
- Benussi A, Karikari TK, Ashton N, Gazzina S, Premi E, Benussi L, et al. Diagnostic and prognostic value of serum NfL and p-Tau181 in frontotemporal lobar degeneration. *J Neurol Neurosurg Psychiatry* 2020; 91: 960–7.
- Bittner T, Zetterberg H, Teunissen CE, Ostlund RE Jr, Militello M, Andreasson U, et al. Technical performance of a novel, fully automated electrochemiluminescence immunoassay for the quantitation of beta-amyloid (1-42) in human cerebrospinal fluid. *Alzheimers Dement* 2016; 12: 517–26.
- Blennow K, Mattsson N, Schöll M, Hansson O, Zetterberg H. Amyloid biomarkers in Alzheimer's disease. *Trends Pharmacol Sci* 2015; 36: 297–309.
- Blennow K, Shaw LM, Stomrud E, Mattsson N, Toledo JB, Buck K, et al. Predicting clinical decline and conversion to Alzheimer's disease or dementia using novel Elecsys Abeta(1-42), pTau and tTau CSF immunoassays. *Sci Rep* 2019; 9: 19024.
- Braak H, Alafuzoff I, Arzberger T, Kretschmar H, Del Tredici K. Staging of Alzheimer disease-associated neurofibrillary pathology using paraffin sections and immunocytochemistry. *Acta Neuropathol* 2006; 112: 389–404.
- Brier MR, Gordon B, Friedrichsen K, McCarthy J, Stern A, Christensen J, et al. Tau and Abeta imaging, CSF measures, and cognition in Alzheimer's disease. *Sci Transl Med* 2016; 8: 338ra66.
- Budgeon CA, Murray K, Turlach BA, Baker S, Villemagne VL, Burnham SC, for the Alzheimer's Disease Neuroimaging Initiative. Constructing longitudinal disease progression curves using sparse, short-term individual data with an application to Alzheimer's disease. *Statist Med* 2017; 36: 2720–34.
- Caballero MAA, Song Z, Rubinski A, Duering M, Dichgans M, Park DC, et al. Age-dependent amyloid deposition is associated with white matter alterations in cognitively normal adults during the adult life span. *Alzheimer's Dement* 2020; 16: 651–61.
- Congdon EE, Sigurdsson EM. Tau-targeting therapies for Alzheimer disease. *Nat Rev Neurol* 2018; 14: 399–415.
- De Felice FG, Wu D, Lambert MP, Fernandez SJ, Velasco PT, Lacor PN, et al. Alzheimer's disease-type neuronal tau hyperphosphorylation induced by A beta oligomers. *Neurobiol Aging* 2008; 29: 1334–47.
- Dubois B, Feldman HH, Jacova C, Hampel H, Molinuevo JL, Blennow K, et al. Advancing research diagnostic criteria for Alzheimer's disease: the IWG-2 criteria. *Lancet Neurol* 2014; 13: 614–29.
- Gonzalez-Escamilla G, Lange C, Teipel S, Buchert R, Grothe MJ. Alzheimer's Disease Neuroimaging I. PETPVE12: an SPM toolbox for Partial Volume Effects correction in brain PET - Application to amyloid imaging with AV45-PET. *Neuroimage* 2017; 147: 669–77.
- Graff-Radford J, Arenaza-Urquijo EM, Knopman DS, Schwarz CG, Brown RD, Rabinstein AA, et al. White matter hyperintensities: relationship to amyloid and tau burden. *Brain* 2019; 142: 2483–91.
- Grothe MJ, Barthel H, Sepulcre J, Dyrba M, Sabri O, Teipel SJ, for the Alzheimer's Disease Neuroimaging Initiative. In vivo staging of regional amyloid deposition. *Neurology* 2017; 89: 2031–8.
- Hanseeuw BJ, Betensky RA, Jacobs HIL, Schultz AP, Sepulcre J, Becker JA, et al. Association of amyloid and tau with cognition in preclinical Alzheimer disease: a longitudinal study. *JAMA Neurol* 2019; 76: 915.
- Hanseeuw BJ, Betensky RA, Mormino EC, Schultz AP, Sepulcre J, Becker JA, et al.; for the Alzheimer's Disease Neuroimaging Initiative. PET staging of amyloidosis using striatum. *Alzheimers Dement* 2018; 14: 1281–92.
- Hansson O, Seibyl J, Stomrud E, Zetterberg H, Trojanowski JQ, Bittner T, et al.; for the Swedish BioFINDER study group. CSF biomarkers of Alzheimer's disease concord with amyloid-beta PET and predict clinical progression: a study of fully automated immunoassays in BioFINDER and ADNI cohorts. *Alzheimers Dement* 2018; 14: 1470–81.
- Hyman BT, Phelps CH, Beach TG, Bigio EH, Cairns NJ, Carrillo MC, et al. National Institute on Aging-Alzheimer's Association guidelines for the neuropathologic assessment of Alzheimer's disease. *Alzheimers Dement* 2012; 8: 1–13.
- Jack CR Jr. The transformative potential of plasma phosphorylated tau. *Lancet Neurol* 2020; 19: 373–4.
- Jack CR Jr, Barnes J, Bernstein MA, Borowski BJ, Brewer J, Clegg S, et al. Magnetic resonance imaging in Alzheimer's Disease Neuroimaging Initiative 2. *Alzheimers Dement* 2015; 11: 740–56.
- Jack CR Jr, Wiste HJ, Lesnick TG, Weigand SD, Knopman DS, Vemuri P, et al. Brain beta-amyloid load approaches a plateau. *Neurology* 2013; 80: 890–6.
- Jack CR Jr, Wiste HJ, Weigand SD, Therneau TM, Lowe VJ, Knopman DS, et al. Defining imaging biomarker cut points for brain aging and Alzheimer's disease. *Alzheimers Dement* 2017; 13: 205–16.
- Jagust WJ, Landau SM, Koeppe RA, Reiman EM, Chen K, Mathis CA, et al. The Alzheimer's disease neuroimaging initiative 2 PET core: 2015. *Alzheimers Dement* 2015; 11: 757–71.
- Janelidze S, Mattsson N, Palmqvist S, Smith R, Beach TG, Serrano GE, et al. Plasma P-tau181 in Alzheimer's disease: relationship to other biomarkers, differential diagnosis, neuropathology and longitudinal progression to Alzheimer's dementia. *Nat Med* 2020; 26: 379–86.
- Jin M, Shepardson N, Yang T, Chen G, Walsh D, Selkoe DJ. Soluble amyloid beta-protein dimers isolated from Alzheimer cortex directly induce Tau hyperphosphorylation and neuritic degeneration. *Proc Natl Acad Sci USA* 2011; 108: 5819–24.
- Johnson KA, Schultz A, Betensky RA, Becker JA, Sepulcre J, Rentz D, et al. Tau positron emission tomographic imaging in aging and early Alzheimer disease. *Ann Neurol* 2016; 79: 110–9.
- Kang JH, Korecka M, Figurski MJ, Toledo JB, Blennow K, Zetterberg H, et al.; Alzheimer's Disease Neuroimaging Initiative. The Alzheimer's disease neuroimaging initiative 2 biomarker core: a review of progress and plans. *Alzheimers Dement* 2015; 11: 772–91.
- Karikari TK, Pascoal TA, Ashton NJ, Janelidze S, Benedet AL, Rodriguez JL, et al. Blood phosphorylated tau 181 as a biomarker for Alzheimer's disease: a diagnostic performance and prediction modelling study using data from four prospective cohorts. *Lancet Neurol* 2020; 19: 422–33.
- Klunk WE, Koeppe RA, Price JC, Benzinger TL, Devous MD Sr, Jagust WJ, et al. The Centiloid Project: standardizing quantitative amyloid plaque estimation by PET. *Alzheimers Dement* 2015; 11: 1-15.e1–15.e4.
- La Joie R, Ayakta N, Seeley WW, Borys E, Boxer AL, DeCarli C, et al. Multisite study of the relationships between antemortem [(11)C]PIB-PET Centiloid values and postmortem measures of Alzheimer's disease neuropathology. *Alzheimers Dement* 2019; 15: 205–16.
- Landau SM, Breault C, Joshi AD, Pontecorvo M, Mathis CA, Jagust WJ, et al. Amyloid-beta imaging with Pittsburgh compound B and florbetapir: comparing radiotracers and quantification methods. *J Nucl Med* 2013; 54: 70–7.
- Lantero Rodriguez J, Karikari TK, Suarez-Calvet M, Troakes C, King A, Emersic A, et al. Plasma p-tau181 accurately predicts Alzheimer's

- disease pathology at least 8 years prior to post-mortem and improves the clinical characterisation of cognitive decline. *Acta Neuropathol* 2020; 140: 267–278.
- Maass A, Landau S, Baker SL, Horng A, Lockhart SN, La Joie R, et al. Comparison of multiple tau-PET measures as biomarkers in aging and Alzheimer's disease. *Neuroimage* 2017; 157: 448–63.
- Mattsson-Carligen N, Andersson E, Janelidze S, Ossenkoppele R, Insel P, Strandberg O, et al. Aβ deposition is associated with increases in soluble and phosphorylated tau that precede a positive Tau PET in Alzheimer's disease. *Sci Adv* 2020; 6: eaaz2387.
- Mattsson N, Andreasson U, Zetterberg H, Blennow K; for the Alzheimer's Disease Neuroimaging Initiative. Alzheimer's disease neuroimaging I. Association of plasma neurofilament light with neurodegeneration in patients with Alzheimer disease. *JAMA Neurol* 2017; 74: 557–66.
- Mattsson N, Cullen NC, Andreasson U, Zetterberg H, Blennow K. Association between longitudinal plasma neurofilament light and neurodegeneration in patients with Alzheimer disease. *JAMA Neurol* 2019; 76: 791–9.
- Mattsson N, Zetterberg H, Janelidze S, Insel PS, Andreasson U, Stomrud E, et al. Plasma tau in Alzheimer disease. *Neurology* 2016; 87: 1827–35.
- Meyer PF, Pichet Binette A, Gonneaud J, Breitner JCS, Villeneuve S. Characterization of Alzheimer disease biomarker discrepancies using cerebrospinal fluid phosphorylated tau and AV1451 positron emission tomography. *JAMA Neurol* 2020; 77: 508–16.
- Mielke MM, Hagen CE, Wennberg AMV, Airey DC, Savica R, Knopman DS, et al. Association of plasma total tau level with cognitive decline and risk of mild cognitive impairment or dementia in the mayo clinic study on aging. *JAMA Neurol* 2017; 74: 1073–80.
- Mielke MM, Hagen CE, Xu J, Chai X, Vemuri P, Lowe VJ, et al. Plasma phospho-tau181 increases with Alzheimer's disease clinical severity and is associated with tau- and amyloid-positron emission tomography. *Alzheimers Dement* 2018; 14: 989–97.
- Moscoso A, Rey-Bretal D, Silva-Rodríguez J, Aldrey JM, Cortes J, Pias-Peleiteiro J, et al. White matter hyperintensities are associated with subthreshold amyloid accumulation. *Neuroimage* 2020; 218: 116944.
- Nakamura A, Kaneko N, Villemagne VL, Kato T, Doecke J, Dore V, et al. High performance plasma amyloid-beta biomarkers for Alzheimer's disease. *Nature* 2018; 554: 249–54.
- O'Connor A, Karikari TK, Poole T, Ashton NJ, Lantero Rodriguez J, Khatun A, et al. Plasma phospho-tau181 in presymptomatic and symptomatic familial Alzheimer's disease: a longitudinal cohort study. *Mol Psychiatry* 2020.
- Ossenkoppele R, Rabinovici GD, Smith R, Cho H, Scholl M, Strandberg O, et al. Discriminative Accuracy of [18F]flortaucipir Positron Emission Tomography for Alzheimer Disease vs Other Neurodegenerative Disorders. *JAMA* 2018; 320: 1151–62.
- Palmqvist S, Insel PS, Stomrud E, Janelidze S, Zetterberg H, Brix B, et al. Cerebrospinal fluid and plasma biomarker trajectories with increasing amyloid deposition in Alzheimer's disease. *EMBO Mol Med* 2019; 11: e11170.
- Palmqvist S, Janelidze S, Quiroz YT, Zetterberg H, Lopera F, Stomrud E, et al. Discriminative Accuracy of Plasma Phospho-tau217 for Alzheimer Disease vs Other Neurodegenerative Disorders. *JAMA* 2020; 324: 772.
- Palmqvist S, Scholl M, Strandberg O, Mattsson N, Stomrud E, Zetterberg H, et al. Earliest accumulation of beta-amyloid occurs within the default-mode network and concurrently affects brain connectivity. *Nat Commun* 2017; 8: 1214.
- Petersen RC, Aisen PS, Beckett LA, Donohue MC, Gamst AC, Harvey DJ, et al. Alzheimer's Disease Neuroimaging Initiative (ADNI): clinical characterization. *Neurology* 2010; 74: 201–9.
- Rabinovici GD, Gatsonis C, Apgar C, Chaudhary K, Gareen I, Hanna L, et al. Association of amyloid positron emission tomography with subsequent change in clinical management among medicare beneficiaries with mild cognitive impairment or dementia. *JAMA* 2019; 321: 1286–94.
- Risacher SL, Fandos N, Romero J, Sherriff I, Pesini P, Saykin AJ, et al. Plasma amyloid beta levels are associated with cerebral amyloid and tau deposition. *Alzheimer's Dement* 2019; 11: 510–9.
- Schindler SE, Bollinger JG, Ovod V, Mawuenyega KG, Li Y, Gordon BA, et al. High-precision plasma beta-amyloid 42/40 predicts current and future brain amyloidosis. *Neurology* 2019; 93: e1647–59.
- Schindler SE, Gray JD, Gordon BA, Xiong C, Batrla-Utermann R, Quan M, et al. Cerebrospinal fluid biomarkers measured by Elecsys assays compared to amyloid imaging. *Alzheimers Dement* 2018; 14: 1460–9.
- Schöll M, Lockhart SN, Schonhaut DR, O'Neil JP, Janabi M, Ossenkoppele R, et al. PET imaging of tau deposition in the aging human brain. *Neuron* 2016; 89: 971–82.
- Schöll M, Maass A, Mattsson N, Ashton NJ, Blennow K, Zetterberg H, et al. Biomarkers for tau pathology. *Mol Cell Neurosci* 2019; 97: 18–33.
- Shaw LM, Waligorska T, Fields L, Korecka M, Figurski M, Trojanowski JQ, et al. Derivation of cutoffs for the Elecsys((R)) amyloid beta (1-42) assay in Alzheimer's disease. *Alzheimer's Dement* 2018; 10: 698–705.
- Shin RW, Ogino K, Shimabuku A, Taki T, Nakashima H, Ishihara T, et al. Amyloid precursor protein cytoplasmic domain with phospho-Thr668 accumulates in Alzheimer's disease and its transgenic models: a role to mediate interaction of Aβ and tau. *Acta Neuropathol* 2007; 113: 627–36.
- Sperling RA, Rentz DM, Johnson KA, Karlawish J, Donohue M, Salmon DP, et al. The A4 study: stopping AD before symptoms begin? *Sci Transl Med* 2014; 6: 228fs13.
- Thal DR, Rub U, Orantes M, Braak H. Phases of Aβ deposition in the human brain and its relevance for the development of AD. *Neurology* 2002; 58: 1791–800.
- Thijssen EH, La Joie R, Wolf A, Strom A, Wang P, Iaccarino L, et al.; Advancing Research and Treatment for Frontotemporal Lobar Degeneration (ARTFL) investigators. Diagnostic value of plasma phosphorylated tau181 in Alzheimer's disease and frontotemporal lobar degeneration. *Nat Med* 2020; 26: 387–97.
- Thomas BA, Erlandsson K, Modat M, Thurfjell L, Vandenberghe R, Ourselin S, et al. The importance of appropriate partial volume correction for PET quantification in Alzheimer's disease. *Eur J Nucl Med Mol Imaging* 2011; 38: 1104–19.
- Vergallo A, Megret L, Lista S, Cavedo E, Zetterberg H, Blennow K, et al.; and the INSIGHT-preAD study group. Plasma amyloid beta 40/42 ratio predicts cerebral amyloidosis in cognitively normal individuals at risk for Alzheimer's disease. *Alzheimers Dement* 2019; 15: 764–75.
- Villemagne VL, Burnham S, Bourgeat P, Brown B, Ellis KA, Salvado O, et al. Amyloid beta deposition, neurodegeneration, and cognitive decline in sporadic Alzheimer's disease: a prospective cohort study. *Lancet Neurol* 2013; 12: 357–67.
- Villemagne VL, Pike KE, Chetelat G, Ellis KA, Mulligan RS, Bourgeat P, et al. Longitudinal assessment of Aβ and cognition in aging and Alzheimer disease. *Ann Neurol* 2011; 69: 181–92.
- Willems EAJ, Maurik IS, Tijms BM, Bouwman FH, Franke A, Hubeek I, et al. Diagnostic performance of Elecsys immunoassays for cerebrospinal fluid Alzheimer's disease biomarkers in a nonacademic, multicenter memory clinic cohort: the ABIDE project. *Alzheimer's Dement* 2018; 10: 563–72.
- Zetterberg H. Blood-based biomarkers for Alzheimer's disease—an update. *J Neurosci Methods* 2019; 319: 2–6.
- Zheng WH, Bastianetto S, Mennicken F, Ma W, Kar S. Amyloid beta peptide induces tau phosphorylation and loss of cholinergic neurons in rat primary septal cultures. *Neuroscience* 2002; 115: 201–11.